Modeling of Asphaltene and Water Associations in Petroleum Reservoir Fluids Using Cubic-Plus-Association EOS

Wenlong Jia
School of Petroleum Engineering, Southwest Petroleum University, Chengdu 610500, People's Republic of China

Ryosuke Okuno
Dept. of Petroleum and Geosystems Engineering, The University of Texas at Austin, Austin, TX 78712

DOI 10.1002/aic.16191
Published online May 3, 2018 in Wiley Online Library (wileyonlinelibrary.com)

Asphaltene is a group of complex compounds commonly present in petroleum reservoir fluids. It is conceivable that asphaltenes strongly interact with water through hydrogen bonding, affecting phase behavior of water/oil mixtures with/without forming an asphaltene-rich phase. In this research, the cubic-plus-association equation of state (CPA EOS) is applied to multiphase behavior resulting from self- and cross-associations of asphaltenes and water in petroleum fluids. This article also presents a new correlation for binary interaction parameters for water with n-alkanes for the CPA EOS by using three-phase data for water/n-alkane binaries. A method is proposed to characterize mixtures of asphaltene-containing oil with water using the CPA EOS. Results show that the CPA EOS can represent multiphase behavior for water/oil mixtures with up to four equilibrium phases: asphaltene-rich, solvent-rich, aqueous, and vapor phases. Case studies include bitumen/water mixtures, involving asphaltene-water emulsion, water solution in bitumen, and their continuous transition with varying temperature. © 2018 American Institute of Chemical Engineers *AIChE J*, 64: 3429–3442, 2018

Keywords: petroleum fluids, asphaltene, asphaltene-water association, cubic-plus-association equation of state, multiphase equilibria

Introduction

Cubic equations of state (EOSs) have been widely used for modeling petroleum reservoir fluids because of their simplicity, computational efficiency, and accuracy for vapor-liquid equilibrium for hydrocarbon mixtures. They were also shown to represent relatively complex multiphase behavior; for example, vapor, solvent-rich liquid, and oleic phases for solvent/oil mixtures.[1–15] The most widely used EOSs in the petroleum industry include the Peng-Robinson (PR) EOS,[16,17] the Soave-Redlich-Kwong (SRK) EOS,[18] and their variants. These equations have been used also in compositional reservoir simulators to solve for phase behavior on the fly.[19,20] The application in compositional flow simulation is probably the most important reason for the necessity for simple EOSs in the petroleum industry.

One of the known limitations in cubic EOS is that they are originally not designed to represent complex phase behavior associated with polar components,[16,18] such as water and asphaltene. These polar components are quite common in oil reservoirs, especially in viscous-oil reservoirs.[21,22] Modeling of them is important when they affect oil-recovery mechanisms and processes; for example, asphaltene precipitation/deposition during CO_2 injection and coinjection of steam and solvent for heavy-oil/bitumen recovery.[11,23,24] In many practical applications, a simple cubic EOS does not offer sufficient flexibility for capturing phase behavior that is more complex than vapor-liquid-liquid equilibrium[25]; for example, asphaltene precipitation, water-asphaltene emulsion, and water dissolution. Modeling such complexities in addition to the hydrocarbon vapor-liquid-liquid equilibrium requires including additional mechanistic parameters that account for hydrogen bonding in an EOS.

The cubic-plus-association (CPA) EOS developed by Kontogeorgis et al.[26] has been shown to be an effective way to model reservoir fluids including polar components. The CPA EOS consists of the physical and association parts. Without associating components in the mixture of interest, the CPA EOS naturally reduces to the cubic EOS, which is the SRK EOS in Kontogeorgis et al.[26] In this research, the CPA EOS based on the SRK EOS is applied to model the association between asphaltene and water in heavy-oil/bitumen reservoir fluids. The central hypothesis in this research is that the CPA EOS can represent complex multiphase behavior for mixtures of water and heavy-oil/bitumen more accurately than the traditional cubic EOS in a mechanistic manner. In case studies, the CPA EOS is applied to experimental phase behavior data that were not accurately represented by the PR EOS in previous publications.

The CPA EOS has been used to model asphaltene phase behavior. Li and Firoozabadi[27,28] presented a unified theoretical framework to predict the asphaltene saturation and onset

Correspondence concerning this article should be addressed to R. Okuno at okuno@utexas.edu

pressures, the amount of precipitated asphaltene, and coexistence of gas, oil and asphaltene phases in gas/oil mixtures by use of the CPA EOS based on the PR EOS. Shirani et al.[29] calculated the asphaltene deposition amount in live oils by use of the CPA EOS. Zhang et al.[30] calculated the asphaltene phase boundary over a wide pressure-temperature (P-T) range with the CPA EOS. Zhang et al.[30] also compared the CPA EOS with the EOS based on perturbed-chain statistical association fluid theory (PC-SAFT). AlHammadi et al.[31] stated that the CPA and PC-SAFT EOSs gave reasonable predictions on the asphaltene onset pressures and precipitation. Arya et al.[32] presented that the CPA EOS was able to correlate the onset pressures of asphaltene, and asphaltene P-T phase envelopes for different amounts of gas injection. Nasrabadi et al.[22] also studied the effect of CO_2 injection on the amount and composition of the asphaltene-rich phase by using the CPA EOS in 2-D and 3-D compositional reservoir simulation models. They found that use of the CPA EOS enabled to model multicomponent asphaltene-rich phase, while the traditional asphaltene models assumed a pure-asphaltene phase.

Besides asphaltene precipitation, the CPA EOS was used to study mutual solubility between water and condensate reservoir fluids by Yan et al.,[33] in which the reservoir fluids were assumed to contain no polar components. Zirrahi et al.[34] calculated the water solubility in petroleum fluids by use of the CPA EOS. Their models included the self-association of water molecules, but the cross-association between water and hydrocarbon components (e.g., asphaltene) was not included.

Previous publications indicate that the CPA EOS has been successfully applied individually to asphaltene precipitation and to aqueous-phase modeling. However, the CPA EOS has not been applied to mixtures of water with asphaltene-containing reservoir fluids in the literature. The main objective of this research is to study the applicability of the CPA EOS to multiphase behavior resulting from associations of water and asphaltene in asphaltene-containing fluids, such as heavy-oil and bitumen.

In what follows, a brief introduction of the CPA EOS is followed by a new correlation developed for binary interaction parameters (BIPs) of water with hydrocarbons. Then, the oil characterization method applied in this research is described. After that, associations of water and asphaltene molecules as well as their effect on multiphase behavior of petroleum reservoir fluids are studied in case studies.

It is beyond the scope of the current paper to compare the CPA EOS with the SRK EOS with the Huron-Vidal mixing rule. Comparisons between the two models for various mixtures of hydrogen bonding compounds can be found in Kontogeorgis and Folas.[35]

Cubic-Plus-Association EOS

The CPA EOS developed by Kontogeorgis et al.[26] is used in this research. When the physical part is based on the Soave-Redlich-Kwong (SRK) EOS,[18,26] the CPA EOS can be expressed as follows

$$P=\frac{RT}{v-b}-\frac{a}{v(v+b)}-\frac{1}{2}\frac{RT}{v}\left(1+v\frac{\partial \ln g}{\partial v}\right) \quad \sum_i x_i \sum_{A_i}(1-X_{A_i})\ \ i=1,2,\ \ldots,\ n_{\text{assoc}} \tag{1}$$

where P is pressure; T is temperature; x is mole fraction; v is molar volume; R is the universal gas constant; n_{assoc} is the total number of association components; A_i is the active association site A on molecule i; X_{A_i} is the fraction of sites A on component i that do not form bonds with other active sites; Σ_i refers to the summation over all components; Σ_{Ai} refers to the summation over all sites (A_i, B_i, C_i) on component i; g is the hard sphere radial distribution function (RDF) determined by

$$g=\frac{1}{1-1.9\eta}, \text{where } \eta=\frac{b}{4v} \tag{2}$$

Calculation of X_{A_i} requires the association strength $\Delta^{A_iB_j}$ between association sites belonging to different molecules. That is

$$X_{A_i}=\frac{1}{1+\rho\sum_j x_j \sum_{B_j}\Delta^{A_iB_j}}\ \ i,j=1,2,\ \ldots,\ n_{\text{assoc}} \tag{3}$$

where ρ is molar density. $\Delta^{A_iB_j}$ is given by Chapman et al.[36] as

$$\Delta^{A_iB_j}=g\left[\exp\left(\frac{\varepsilon^{A_iB_j}}{RT}\right)-1\right]b_{ij}\beta^{A_iB_j} \tag{4}$$

$$b_{ij}=\frac{b_i+b_j}{2} \tag{5}$$

where $\varepsilon^{A_iB_j}$ is the association energy (the potential square-well depth) for the association between A_i and B_j; $\beta^{A_iB_j}$ is the association volume that represents the finite distance (the potential square-well width) at which the inter-particle potential between A_i and B_j is zero; b is the co-volume.

The energy parameter a in Eq. 1 is given by

$$a=a_0\left[1+\kappa\left(1-\sqrt{T_r}\right)\right]^2 \tag{6}$$

This contributes to the physical part based on the SRK EOS in Eq. 1.

For a pure associating component, there are five parameters (a_0, b, κ, $\varepsilon^{A_iB_j}$, and $\beta^{A_iB_j}$) in the CPA EOS. They are typically determined by fitting the EOS to vapor pressures and liquid densities measured for the pure component. For inert (non-self-associating) components, only three parameters (a_0, b, and κ) are required, which can be calculated from the critical temperature (T_c), critical pressure (P_c), and acentric factor (ω) for the component of interest.[35]

When the CPA EOS is applied to a mixture, the van der Waals mixing rules are employed for a and b in the physical part; that is

$$a=\sum_i\sum_j x_i x_j a_{ij} \tag{7}$$

$$a_{ij}=\sqrt{a_i a_j}\left(1-k_{ij}\right) \tag{8}$$

$$b=\sum_i x_i b_i \tag{9}$$

where k_{ij} is the BIP for components i and j. k_{ij} is the only binary adjustable parameter of the CPA EOS.

The $\varepsilon^{A_iB_j}$ and $\beta^{A_iB_j}$ parameters for a mixture are calculated from the CR-1 combining rule[35] as follows

$$\beta^{A_iB_j}=\sqrt{\beta^{A_iB_i}\beta^{A_jB_j}} \tag{10}$$

$$\varepsilon^{A_iB_j}=\frac{\varepsilon^{A_iB_i}+\varepsilon^{A_jB_j}}{2} \tag{11}$$

Some inert compounds that do not form self-association are considered to form cross-association with other self-association compounds, forming "solvating mixtures"[35,37]; for example, mixtures of aromatic hydrocarbons with water. The

CR-1 combining rule is also suitable for solvating mixtures, in which the $\varepsilon^{A_iB_j}$ parameter for the inert compound is set to zero while $\beta^{A_iB_j}$ for the inert compound is adjusted to match experimental data for multiphase equilibrium, such as vapor-liquid, liquid-liquid, and vapor-liquid-liquid.

In order to solve the CPA EOS, the CPA EOS is expressed in terms of compressibility factor $Z=Pv/RT$. Then, Eq. 1 can be written as

$$Z=\frac{Z}{Z-B}-\frac{AZ}{(Z+B)Z}-\frac{0.5Z}{Z-0.475B}\sum_i x_i\sum_{A_i}(1-X_{A_i}) \quad (12)$$

$$X_{A_i}=\frac{Z}{Z+\sum_j x_j\sum_{B_j}\gamma^{A_iB_j}} \quad (13)$$

where $A=aP/R^2T^2$, $B=bP/RT$, and $\gamma^{A_iB_j}=P\Delta^{A_iB_j}/RT$. Eq. 12 is highly nonlinear mainly because of X_{A_i}. The bisection method and Newton's method are recommended to solve the CPA EOS by Michelsen.[38] Equation 12 typically has one to three real roots. In the case of more than one real root, the compressibility factor that gives the lowest Gibbs free energy is selected.[22]

The fugacity coefficient for the CPA EOS is as follows

$$\ln\varphi_i=-\ln(Z-B)+\frac{b_i}{b}\left(\frac{Z}{Z-B}-\frac{AZ}{(Z+B)Z}\right)-\frac{A}{B}\left(\frac{2\sum_j x_j a_{ij}}{a}-\frac{b_i}{b}\right)\ln\left(\frac{Z+B}{Z}\right)+\sum_{A_i}\ln X_{A_i}-\frac{1}{2}\sum_i x_i\sum_{A_i}(1-X_{A_i})\frac{\partial\ln g}{\partial x_i} \quad (14)$$

where

$$\frac{\partial\ln g}{\partial x_i}=\frac{0.475B}{Z}\left(\frac{Z}{Z-0.475B}\right)\frac{b_i}{b} \quad (15)$$

The CPA EOS is applied to multiphase equilibria, consisting of vapor (V), water-rich (W), asphaltene-rich (L_1), and oil-rich (L_2) phases, in this research. The 4C association scheme[32,35] is used for both water and asphaltene, indicating one water/asphaltene molecule has two electron-donor sites and two electron-acceptor sites for self-association and cross-association. Multiphase flash in this research is based on the method of Michelsen,[39,40] in which phase split and stability calculations are applied in a sequential manner. The algorithm for the solution of multiphase Rachford-Rice equations is based on the method of Okuno et al.[41]

New BIP Correlation for Water with Hydrocarbons for the CPA EOS

In this research, it is of fundamental importance for the CPA EOS to be calibrated for water/*n*-alkane phase behavior. This section presents the development of a new BIP correlation for water with *n*-alkanes for the CPA EOS. The experimental data used are three-phase curves measured for water/*n*-alkane binaries by Brunner.[42] The BIP for water with *n*-alkane in the CPA EOS is the only adjustable parameter in the optimization for each binary. The optimal BIP values for these binaries are then used to make a BIP correlation with respect to *n*-alkane's molecular weight (MW). This procedure is similar to Venkatramani and Okuno,[43] in which a BIP correlation was developed for water with *n*-alkanes on the basis of the PR EOS.

Table 1. The Three-Phase Coexistence Data of Water/*n*-Alkane Binaries Used for the Development of the New BIP Correlation Eq. 16: Experimental Data Were Taken from Brunner[42]

Hydrocarbon	No. of data points	Pressure (kPa)	Temperature (K)
n-C_7	6	1025–5998	429–517
n-C_{10}	6	1473–9655	465–568
n-C_{12}	8	4060–11,340	519–585
n-C_{16}	8	1100–14,270	456–606
n-C_{20}	11	454–15,960	420–617
n-C_{24}	8	1066–14,830	455–612
n-C_{28}	9	4750–21,040	532–639
n-C_{32}	9	2612–20,630	498–639
n-C_{36}	8	6090–21,830	548–644

Phase behavior of water/*n*-alkane binaries is known as Type III in the classification method of Konynenburg and Scott.[3] The oleic-vapor-aqueous (L-V-W) three-phase line represents the boundary between the L-W region and the L-V/W-V regions. It is crucial for a thermodynamic model to be able to accurately represent L-V-W coexistence curves for water/*n*-alkane binaries since three types of two-phase regions (L-W, V-W, and V-L) are originated with the three-phase curve for each water/*n*-alkane binary.[43] The L-V-W coexistence curve is sometimes referred to as the three-phase curve in this article. Unlike the previous BIP correlations that were developed by fitting the CPA EOS to water-oil mutual solubility data, we optimize the BIP for water with *n*-alkane in terms of the three-phase curve. As will be shown later, the resulting BIPs yield accurate predictions of the mutual solubility of water/*n*-alkane mixtures with the CPA EOS.

As summarized in Table 1, the current research uses the data for L-V-W three-phase coexistence curves for water with *n*-C_7, *n*-C_{10}, *n*-C_{12}, *n*-C_{16}, *n*-C_{20}, *n*-C_{24}, *n*-C_{28}, *n*-C_{32}, and *n*-C_{36} presented in Brunner.[42] For each binary, the BIP is adjusted until the difference between the experimental and calculated three-phase temperature is less than 0.1 K for experimental pressures. This optimization was straightforward since the only adjustable parameter, the BIP for each binary, monotonically changes the three-phase curve calculated by the CPA EOS. Figure 1 shows the measured L-V-W three-phase points and the calculated curves by use of the CPA EOS with the BIP

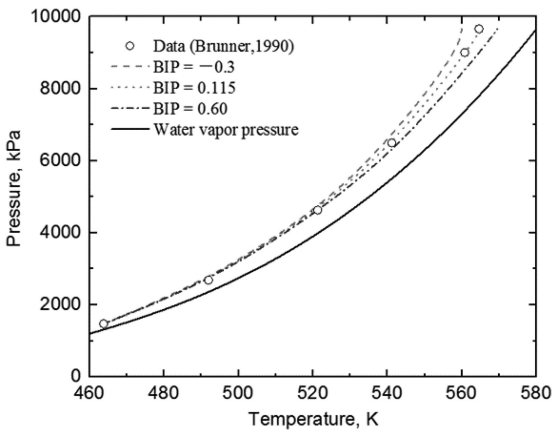

Figure 1. Effect of BIP on the oleic-vapor-aqueous (L-V-W) three-phase curve of water/*n*-C_{12}.

The data were taken from Brunner.[42] The results show that the BIP has a monotonic effect on the three-phase curve.

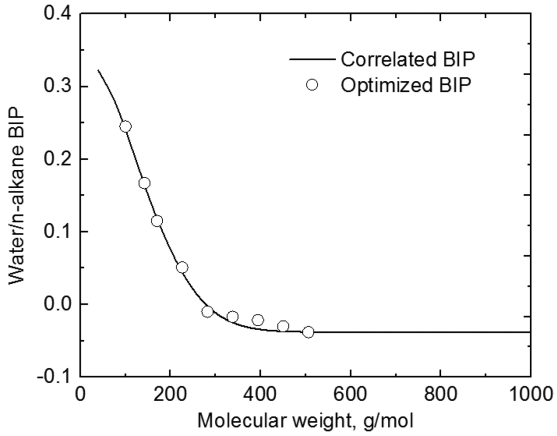

Figure 2. Optimized BIP data and the correlated curve for water/*n*-alkane binaries based on matching three-phase coexistence curves measured by Brunner.[42]

values of −0.3, −0.0685, 0.165, and 0.60 for water/*n*-C_{12}. It is shown that the three-phase curve becomes closer to the water vapor pressure curve with increasing BIP values.

Figure 2 shows that the optimal BIP rapidly decreases with increasing MW until *n*-C_{20}, and then levels off. A similar trend with the PR EOS was obtained by Venkatramani and Okuno,[43] in which the limiting BIP value of 0.242 was determined for water with *n*-alkanes heavier than *n*-C_{26}. This asymptotic trend is related to the experimental observation that the three-phase curve and water solubility in *n*-alkane approach their asymptotic limits as the *n*-alkane component becomes heavier.[42]

Then, the optimized BIPs for water/*n*-alkane binaries are correlated as follows

$$K_{w-HC}=C_1 MW^{\left(C_2 MW^{C_3}\right)} \tag{16}$$

where *MW* is the MW of *n*-alkane, g/mol; $C_1 = 0.38185$, $C_2 = -1.7172 \times 10^{-5}$, $C_3 = 1.7991$. This correlation gives a limiting BIP value of −0.038 for *n*-alkanes heavier than *n*-C_{36}, which enables the CPA EOS to capture the asymptotic behavior of water solubility in *n*-alkane. The range of BIP values calculated from Eq. 16 is reasonable because BIP is usually restricted to be between −1 and 1.[35]

Table 2 shows the optimized BIPs along with the correlated values based on Eq. 16. The average absolute deviation (AAD) between the optimized and correlated data is 0.00472, and the maximum deviation of 0.0125 occurs for *MW* = 394 g/mol. The value of R squared (R^2) for the optimized and correlated values is 0.99839. The standard deviation of Eq. 16 is 0.0974 when it is applied to *n*-alkanes from *n*-C_7 to *n*-C_{36}.

Table 2. Comparison of the Optimized BIPs for Water/*n*-Alkane Binaries with the Correlated Values Based on Eq. 16

Component	*MW* (g/mol)	Optimized BIP	Correlated BIP
n-C_7	100	0.245	0.241
n-C_{10}	142	0.167	0.165
n-C_{12}	170	0.115	0.116
n-C_{16}	226	0.051	0.039
n-C_{20}	282	−0.010	−0.006
n-C_{24}	338	−0.0170	−0.0269
n-C_{28}	394	−0.0215	−0.0340
n-C_{32}	450	−0.0300	−0.0369
n-C_{36}	506	−0.0380	−0.0378
–	2000	–	−0.0380
–	3000	–	−0.0380

The BIP correlation, Eq. 16, was developed by use of L-V-W three-phase P-T points measured by Brunner.[42] The CPA EOS together with Eq. 16 is now tested in terms of predictive capability for the water solubility in *n*-alkanes. Skripka[44] reported water solubilities in liquid hydrocarbons along the oleic-vapor-aqueous (L-V-W) three-phase curve for water/*n*-alkanes binaries with *n*-C_6, *n*-C_7, *n*-C_8, *n*-C_9, *n*-C_{10}, *n*-C_{12}, *n*-C_{16}, and *n*-C_{20}. Water solubilities in *n*-C_6 and *n*-C_8 were given in Heidman et al.[45] and Tsonopoulos and Wilson,[46] respectively. Comparison of the predictions with the experimental data is shown in Figure 3. Table 3 presents the deviation analysis; the maximum AAD is 0.0325 for the mole fraction of water, which is slightly better than the maximum AAD of 0.0420 reported by Venkatramani and Okuno[43] for the PR EOS.

Figure 4 compares the water solubility data and calculation results for the water/*n*-C_7 binary. The calculation results are shown for three models; the CPA EOS with the new BIP correlation (Eq. 16), the PR EOS with the BIP correlation by Venkatramani and Okuno,[43] and the CPA EOS with the BIP correlation by Folas et al.[37]

$$K_{w-HC}=-0.026\times CN+0.1915 \tag{17}$$

where *CN* refers to the carbon number of *n*-alkane. This correlation was developed by matching the liquid-liquid equilibrium data for water/*n*-alkanes from propane up to decane. The BIP for water with *n*-C_7 for the CPA EOS is 0.2410 with Eq. 16, and 0.0095 with Eq. 17.

The CPA EOS with Eq. 16 yields the AAD of 0.0256 for water mole fraction dissolved in *n*-C_7. The AAD for the same set of data is 0.0471 with the CPA EOS with Folas et al.'s BIP correlation, and 0.0353 with the PR EOS with Venkatramani and Okuno's BIP correlation.

Figure 5 presents the monotonic and asymptotic behavior of the three-phase coexistence curve and water solubility in *n*-alkane when the CPA EOS is used with Eq. 16 for water/*n*-alkane binary interaction. For *n*-C_{100}, the three-phase curve only slightly deviates from the vapor pressure of water. The water-solubility plot shows Type IIIa for water/*n*-C_{10}, but Type IIIb for water/*n*-C_{36} and/*n*-C_{100}, which is consistent with experimental data.[42]

Equation 16 can be used with the CPA EOS for nonpolar hydrocarbons, although the development is based on data for *n*-alkane/water binaries. This is because the CPA EOS represents the solubility of water in aromatics as solvation, for which β^{AB} for aromatic components are adjusted to match experimental data. The solvation method accounts for the cross-association between water and aromatic hydrocarbons, which results in more water dissolved in aromatics than in the homomorph *n*-alkane.[45,46] On the basis of the CPA EOS, Folas et al.[37] presented that, for water/aromatic hydrocarbon mixtures, the BIPs for water/*n*-alkane binaries can be applied to the corresponding homomorph aromatic hydrocarbons (e.g., the BIP value of water with benzene is assumed to be the same as that of water with hexane).[35]

Characterization Method

The main objective of this article is to present the application of the CPA EOS to represent multiphase behavior when asphaltene-containing oil, such as bitumen, is mixed with

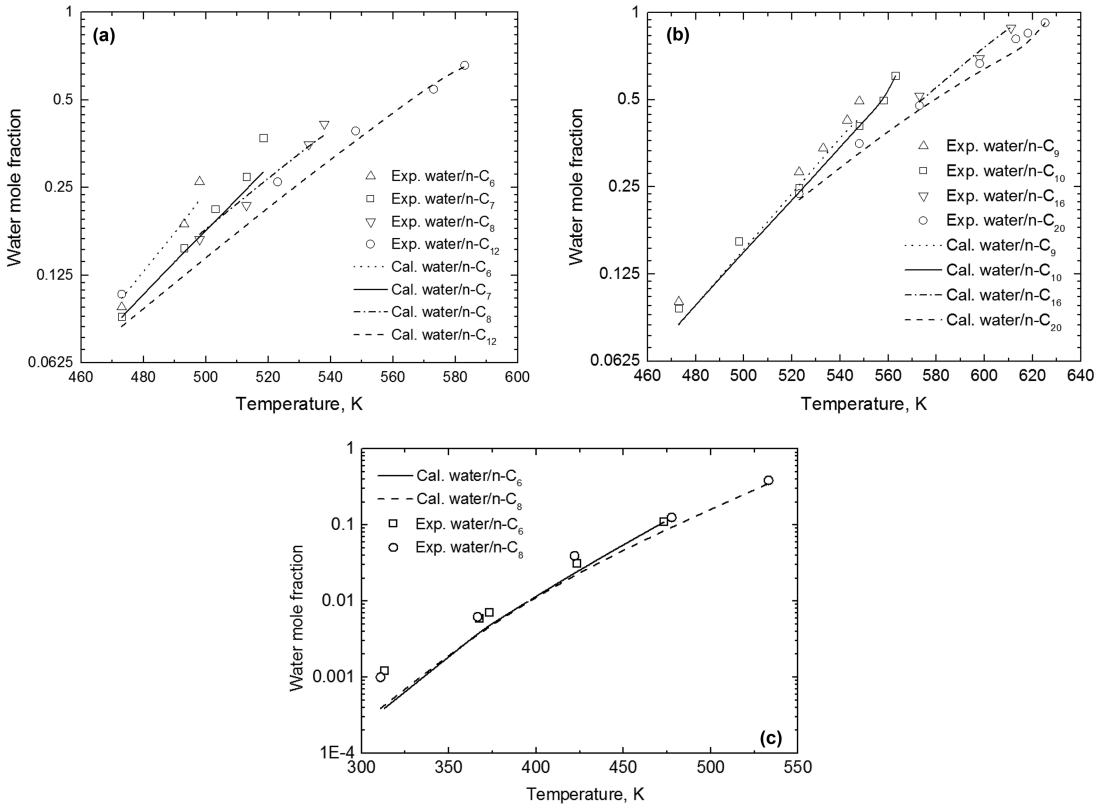

Figure 3. Comparison of predicted water solubilities in *n*-alkanes against experimental data.

(a, b) Experimental data were taken from Skripka[44]; (c) experimental data were taken from Heidman et al.[45] and Tsonopoulos and Wilson.[46]

water. Experimental data available in the literature are used to characterize such oils, and for the comparison with calculated phase behavior by the CPA EOS. The research was motivated by the hypothesis that the association term in the CPA EOS enables to represent multiphase behavior resulting from associations of water and asphaltene while keeping bubble-points that can be accurately modeled by the traditional cubic EOS (e.g., SRK EOS).

For this investigation, the method employed consists of the following main steps:

Step 1. Phase behavior data, such as MW, saturates-aromatics-resins-asphaltene (SARA) composition, bubble points, and liquid densities, are collected for asphaltene-containing oil from the literature. The bubble points used can be those measured for mixtures of gases with the oil to be characterized.

Table 3. Deviation of the Calculations from the Measured Values for Water Solubility in *n*-Alkane Along the Three-Phase Coexistence Curve: the Water Solubility is Represented by the Mole Fraction of Water in the Liquid Phase

Hydrocarbon	Number of data points	T range (K)	AAD in water solubility	Data sources
n-C_6	8	313–498	0.0072	44, 46
n-C_7	4	473–513	0.0122	44, 45
n-C_8	9	310–538	0.0160	44
n-C_9	5	473–548	0.0325	44
n-C_{10}	6	473–563	0.0073	44
n-C_{12}	5	473–583	0.0214	44
n-C_{16}	3	573–611	0.0261	44
n-C_{20}	7	523–625	0.0323	44

Step 2. The oil is characterized by use of the SRK EOS, in which the PVTsim Nova software, version 3.0[47] is used to match bubble points and liquid densities with four pseudo components. The heaviest pseudo component represents asphaltene, and the other three pseudo components (PC1, PC2, and PC3) collectively represent a mixture of saturates, aromatics, and resins. PC1, PC2, and PC3 are considered as non-self-associating components in this research; that is, their T_C, P_C, and ω based on the SRK EOS can be used directly with

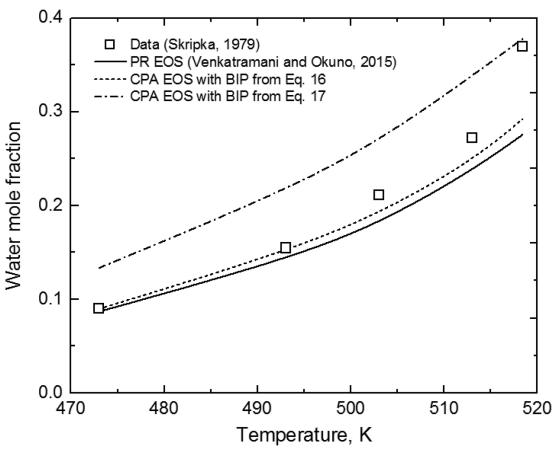

Figure 4. Comparison of the calculated water solubilities in n-C_7 against measured data along the three-phase curve of the water/n-C_7 binary.

The experimental data were taken from Skripka.[44] The BIP for the CPA is 0.2410 with Eq. 16, and 0.0095 with Eq. 17. The BIP for the PR EOS is 0.5529.

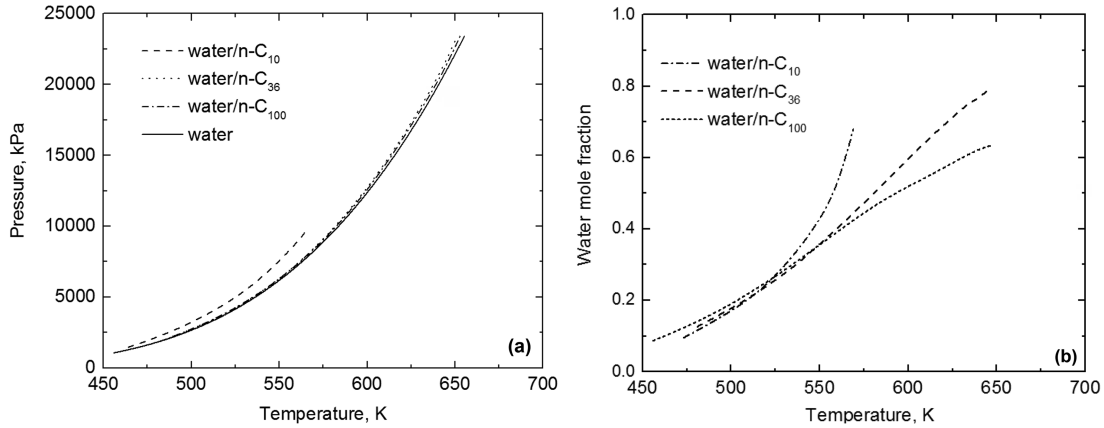

Figure 5. (a) Monotonic and asymptotic trend of the three-phase curves of water/*n*-alkane binaries by use of the CPA EOS; (b) calculated water solubilities in *n*-alkanes along the three-phase curves of water/*n*-alkane binaries by use of the CPA EOS.

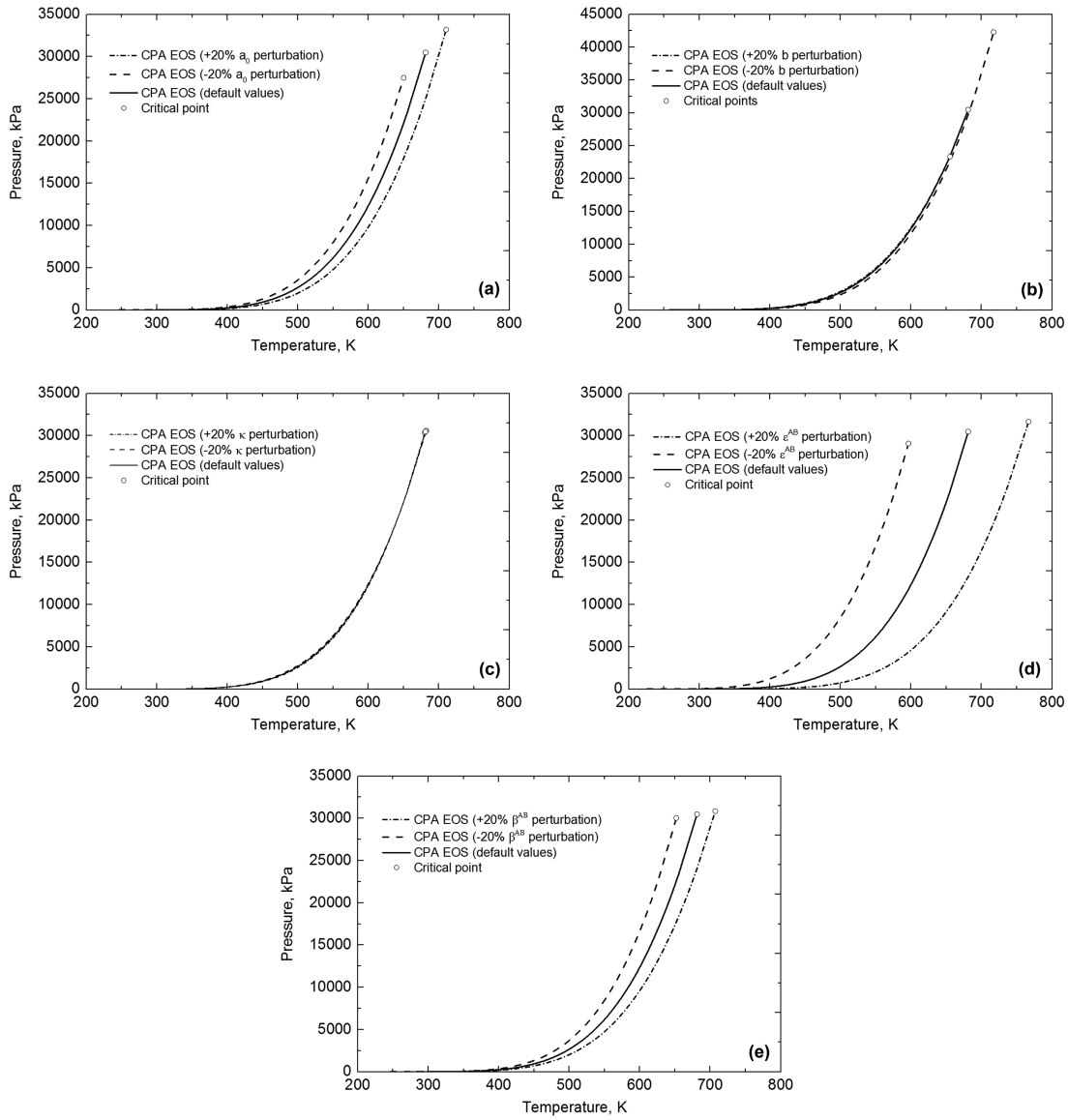

Figure 6. Effect of a_0, b, κ, ε^{AB}, and β^{AB} on the water vapor pressure curve.

The default values for water for the CPA EOS were taken from Kontogeorgis and Folas.[36]

Table 4. Properties of the Athabasca Bitumen for Case 1[a]

Component	z	MW (g/mol)	T_c (K)	P_c (kPa)	ω	β^{AB}	a_0 (kPa·m^6·mol^{-2})	b (m^3·mol^{-1})	κ	ε^{AB} (kPa·m^3·mol^{-1})	$K_{w\text{-}HC}$	Volume shift (m^3/mol)
PC1	0.2664	352.43	612.8	2287.1	0.9673	0.07	–	–	–	–	−0.0293	−0.000013
PC2	0.4925	539.03	745.2	1588.5	1.1751	0.07	–	–	–	–	−0.0378	−0.00012
PC3	0.1360	706.84	858.9	1332.7	1.2018	0.07	–	–	–	–	−0.0380	−0.00026
Asphaltene	0.1041	916.19	1340	941.89	1.5567	0.05	0.05202	0.000914	2.50	26.0	−0.0380	−0.00044

[a]Data given by Badamchi-Zadeh et al.[51] were used to characterize PC1, PC2, PC3, and asphaltene. BIPs are calculated by use of Eq. 16. z indicates the overall composition. P_C and ω are not needed for the asphaltene component in the CPA EOS; they are listed here because they were used in the characterization procedure.

the CPA EOS. The asphaltene pseudo component is the only self-associating component within the oil to be characterized, besides the water component to be added in Step 4.

Step 3. The CPA EOS parameters (a_0, b, κ, ε^{AB}, and β^{AB}) for the asphaltene component are obtained by reproducing the vapor pressure curve, including the critical point that was determined in Step 2. This requires initial guesses for the CPA EOS parameters and iteration of them, as explained below.

The a_0, b, and κ parameters are initialized on the basis of T_C, P_C, and ω for the asphaltene component from Step 2 (based on the SRK EOS). The other two parameters, ε^{AB} and β^{AB}, are initialized based on the research by Li and Firoozabadi[27] and Arya et al.[32]. Li and Firoozabadi[27] presented that ε^{AB} represents the normal hydrogen-bonding in the range of $\varepsilon^{AB}/R = 1500$–$12{,}000$ K. Arya et al.[32] summarized that $\beta^{AB} = 0.05$–0.10 and $\varepsilon^{AB}/R = 1500$–$3000$ K for asphaltene. Furthermore, a fixed β^{AB} value is used for a given asphaltene.[29,30] In this research, β^{AB} is fixed to be 0.05 for the asphaltene component. $\varepsilon^{AB} = 25$ kPa·m^3·mol^{-1} is used as the initial values for the asphaltene component in this step.

The iteration is performed for three parameters a_0, b, and ε^{AB} which substantially affect the vapor pressure calculated by the CPA EOS. The iteration is based on the observations that increasing any one of a_0, ε^{AB} and β^{AB} tends to increase the critical point for a given compound, and that increasing the co-volume parameter b tends to decrease the critical point while keeping the vapor pressures. These observations are demonstrated by use of water as an example in Figure 6. The CPA EOS parameters for water are given by Kontogeorgis and Folas[35] as follows: $a_0 = 0.0001227$ kPa·m^6·mol^{-2}, $b = 0.0000145$ m^3·mol^{-1}, $\kappa = 0.6735$, $\varepsilon^{AB} = 16.655$ kPa·m^3·mol^{-1}, and $\beta^{AB} = 0.0692$.

The reproduction of the vapor pressure from the SRK EOS by use of the CPA EOS in this step does not have to be strict because the asphaltene component's vapor pressure does not contribute to the bubble points of the four-component oil characterized. Also, the properties of the asphaltene component set here are going to be adjusted in the next step, in which ε^{AB} is used to match additional data regarding water/asphaltic-oil interaction, such as water solubilities and emulsion.

Step 4. This step is to study the impact of the association term of the CPA EOS on multiphase behavior associated with water-asphaltene interaction. That is, water becomes part of the EOS model in this step. The association energy ε^{AB} is the only adjustable parameter for the asphaltene component. The β^{AB} parameters for the other three components (PC1, PC2, and PC3) are adjusted to account for the cross-association between water and aromatic hydrocarbons, referred to as solvation.[37] These parameters are adjusted to match one data point; then, predictions from the resulting CPA EOS model are compared with other data points for mixtures of water and asphaltene-containing oil.

The BIPs for water with the hydrocarbon components (i.e., SARA) are not adjusted, and calculated by the new correlation, Eq. 16 (see the previous section). The BIPs between non-self-associating components are set to zero in this research.

Step 5: The volume shift method[48] is applied to match the liquid density used in Step 1.

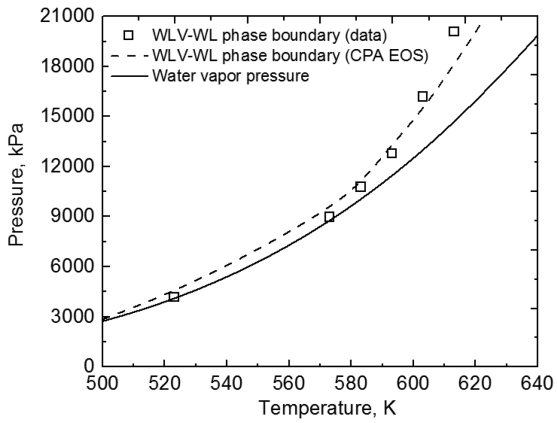

Figure 7. Comparison of measured and calculated WLV-WL phase boundary of the water (55.9 wt %) and Athabasca bitumen (44.1 wt %) mixture for Case 1.

The experimental data are taken from Amani et al.[49]

Case Studies

In this section, the CPA EOS is applied to four different cases, to show the importance of accounting for water-asphaltene associations. The cases include mixtures of water/Athabasca-bitumen, *n*-butane/Athabasca-bitumen/water, water/Peace River bitumen, and toluene/asphaltene/water.

Table 5. Comparison of Experimental and Calculated Water Solubilities in Bitumen for Case 1[a]

T (K)	P (kPa)	Water solubility (data)	Water solubility (CPA EOS)
548.2	6910	0.5412	0.5431
573.1	9520	0.6321	0.6412
583.2	11,550	0.6699	0.6785
593.1	13,480	0.7192	0.7168
603.5	15,320	0.7477	0.7642
613.4	18,450	0.7964	0.7887
623.2	20,930	0.8274	0.8250
633.8	23,720	0.8462	0.8572

[a]The water solubility is presented by the mole fraction. The experimental data were taken from Amani et al.[50] The CPA EOS parameters are given in Table 4.

Table 6. Properties of the *n*-Butane/Bitumen/Water Mixture for Case 2[a]

	z	MW (g/mol)	T_c (K)	P_c (kPa)	ω	β^{AB}	a_0 (kPa·m^6·mol^{-2})	b (m^3·mol^{-1})	κ	ε^{AB} (kPa·m^3·mol^{-1})	$K_{w\text{-}HC}$	Volume shift (m^3/mol)
H_2O	0.6202	18.02	647.3	22,089	0.3440	0.0692	0.00012	0.0000145	0.6735	16.655	0	0
n-C_4H_{10}	0.3702	58.12	425.2	3799.7	0.1930	–	–	–	–	–	0.3062	0.000007
PC1	0.0057	361.2	520.1	1516.2	0.7241	0.02	–	–	–	–	−0.0293	−0.000035
PC2	0.0023	812.4	635.2	1078.5	0.8733	0.02	–	–	–	–	−0.0378	−0.00034
PC3	0.0011	1376	835.8	952.5	1.0609	0.02	–	–	–	–	−0.0380	−0.00070
Asphaltene	0.0005	1757	920.0	752.56	1.14	0.05	0.05694	0.000909	2.05	Equation 18	−0.0380	−0.00121

[a]Pseudo components, PC1, PC2, PC3, and asphaltene, were characterized on the basis of the data given in Gao et al.[25] BIPs are calculated by use of Eq. 16.

Case 1: Water and athabasca bitumen

Amani et al.[49] observed multiphase behavior for mixtures of water with Athabasca bitumen at conditions 522–644 K and 3.9–26.2 MPa. They found that the WLV phase behavior persisted up to the critical temperature of water. They also measured water solubilities in the bitumen-rich phase at WLV-WL transition points.[50]

Characterization of Athabasca bitumen (Steps 2 and 3) uses the data provided by Badamchi-Zadeh et al.[51] The EOS parameters mentioned in Step 4 in the previous section are adjusted to match one data point for the WLV-WL phase boundary. Then, water solubilities predicted by the resulting CPA EOS model are compared with the data. Table 4 summarizes the resulting CPA EOS model for this case.

Figure 7 shows the comparison of experimental and calculated WLV-WL phase boundary. Only the data point at 593.1 K has been matched in Step 4, yielding β^{AB} for PC1, PC2, and PC3, and a_0, b, and ε^{AB} for the asphaltene component as given in Table 4. Based on this one-point calibration, the dashed curve in Figure 7 is predicted. AAD between the experimental and calculated phase transition pressures is 771 kPa. No emulsion phase was reported by Amani et al.[49] The experimental temperatures above 522 K seem to be too high for emulsion.

Table 5 compares the predictions by the CPA EOS model with the measured water solubilities in bitumen-rich phase. The AAD is 0.00745 in terms of water mole fraction. In particular, the CPA EOS model predicts multiphase equilibrium with accurate water solubilities at 623.2 and 633.8 K. However, the PR EOS gave a stable single phase for these conditions in the research by Venkatramani and Okuno,[43] although such high temperatures are unlikely for practical oil-recovery processes.

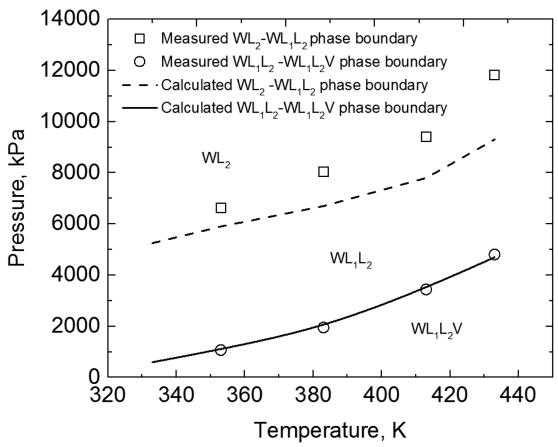

Figure 8. Measured and calculated phase boundaries for the *n*-butane/Athabasca-bitumen/water mixture for Case 2.

The experimental data are taken from Gao et al.[25] The curves are predicted by use of the CPA EOS.

Case 2: n-butane/athabasca-bitumen/water mixtures

Understanding the phase behavior of solvent/bitumen/water mixtures is important for steam-solvent coinjection for *in situ* bitumen recovery.[52–56] However, such mixtures are highly size-asymmetric, and also contain polar components, such as water and asphaltene. It is challenging to model multiphase behavior for them using a single EOS.

Gao et al.[25] measured multiphase behavior of *n*-butane/bitumen/water mixtures, and observed the complex phase transitions from WL_2 to WL_1L_2 to WL_1L_2V with decreasing pressure at temperatures 353–433 K. They showed that the PR EOS was not able to accurately represent the WL_2/WL_1L_2 boundary for 37.02 mol % *n*-butane + 0.96 mol % bitumen + 62.02 mol % water ("Mixture C" in Gao et al.[25]) below 393 K. They observed emulsion for this mixture. In this subsection, the CPA EOS is applied to match the experimental phase boundaries.

The bitumen density and vapor pressure data given in Gao et al.[25] are used to characterize four pseudo components PC1, PC2, PC3, and asphaltene. Table 6 summarizes the parameters for the CPA EOS model. It is not difficult to match the WL_1L_2V/WL_1L_2 boundary (bubble point). This is because the saturation vapor pressure depends mainly on the lighter components in the mixture (i.e., water and *n*-butane), which are not significantly affected by the association properties. Indeed, the PR EOS was shown to successfully represent this phase boundary in Gao et al.[25]

The CPA EOS with a constant ε^{AB} value did not satisfactorily reproduce the WL_1L_2/WL_2 boundary. Matching two WL_1L_2/WL_2 data points at 353.0 and 432.9 K yielded two ε^{AB} values, which were then correlated with temperature. Reasonable representation of the WL_1L_2/WL_2 boundary with the CPA EOS can be achieved by using

$$\varepsilon^{AB} = 13.5 + 0.03125(T - 353) \tag{18}$$

where T is temperature in Kelvin, and ε^{AB} is association energy in kPa·m^3·mol^{-1}. Arya et al.[32] also used a temperature-dependent ε^{AB} to represent asphaltene onset conditions.

Figure 8 shows the comparison of experimental and calculated phase boundaries. The phase labeling in the figure are based on the experimental observation, and also confirmed in the EOS calculations. It is shown that AAD between the measured and calculated WL_1L_2V/WL_1L_2 phase boundary points is 49.3 kPa, and AAD for the WL_1L_2/WL_2 phase boundary points is 1553 kPa. Although the CPA EOS model gives a relatively high AAD for the WL_1L_2/WL_2 phase boundary, this is

Table 7. Flash Results for the *n*-Butane/Athabasca Bitumen/Water Mixture for Case 2[a]

		3400 kPa				3600 kPa			8100 kPa	
Component	z	V	L_1	L_2	W	L_1	L_2	W	L_2	W
H_2O	0.6202	0.07336	0.29203	0.0242	0.99999	0.29002	0.0235	0.99999	0.01996	0.99999
n-C_4H_{10}	0.3702	0.92216	0.52521	0.95221	0.00001	0.52881	0.9531	0.00001	0.95525	0.00001
PC1	0.0057	0.00416	0.00447	0.0148	0	0.00443	0.01469	0	0.01469	0
PC2	0.0023	0.00032	0.00119	0.00603	0	0.00116	0.00597	0	0.00596	0
PC3	0.0011	0	0.00196	0.00275	0	0.00177	0.00272	0	0.00273	0
Asphaltene	0.0005	0	0.17514	0.00002	0	0.17382	0.00003	0	0.00140	0
Phase mole fraction		0.0047	0.0031	0.3825	0.6097	0.0031	0.3867	0.6102	0.3875	0.6125
Phase volume fraction		0.0306	0.0157	0.8181	0.1356	0.0163	0.8425	0.1412	0.8318	0.1682
Density (kg/m^3)		99.40	771.52	369.81	917.51	771.05	377.42	917.63	472.33	920.41

[a]Temperature is 413 K. The CPA EOS parameters are given in Table 6.

Table 8. Properties of Peace River Bitumen Containing Water for Case 3[a]

Component	z	MW (g/mol)	T_C (K)	P_C (kPa)	ω	β^{AB}	a_0 (kPa·m^6·mol^{-2})	b (m^3·mol^{-1})	κ	ε^{AB} (kPa·m^3·mol^{-1})	$K_{w\text{-}HC}$	Volume shit (m^3/mol)
H_2O	0.7481	18.02	647.3	22,088.8	0.3440	0.0692	0.00012	0.0000145	0.6735	16.655	0.000	
PC1	0.0987	262.61	850.3	1658.8	0.8698	0.02	–	–	–	–	0.0060	−0.000002
PC2	0.0698	510.05	919.6	1262.2	1.0925	0.02	–	–	–	–	−0.0378	−0.000021
PC3	0.0544	650.15	957.0	1052.7	1.2266	0.02	–	–	–	–	−0.038	−0.000043
Asphaltene	0.0289	1200.1	992.2	959.1	1.7008	0.05	0.03569	0.000877	2.33	17.50	−0.038	−0.000073

[a]The data given by Mehrotra and Svrcek[58] were used to characterize PC1, PC2, PC3, and asphaltene. BIPs are calculated by use of Eq. 16.

a significant improvement over the PR EOS model by Gao et al.[25]

Table 7 shows detailed flash results regarding WL_1L_2V, WL_1L_2, and WL_2 equilibrium at different pressures at 413 K. The CPA EOS model shows the WL_2 equilibrium at 8100 kPa, in which the W phase is nearly 100% water, and the water mole fraction in the L_2 phase is 1.996%. At 3600 kPa, the L_2 phase is substantially diluted by *n*-butane. Asphaltene does not dissolve in *n*-butane, and therefore, forms another phase, L_1. This asphaltene-rich L_1 phase contains water because

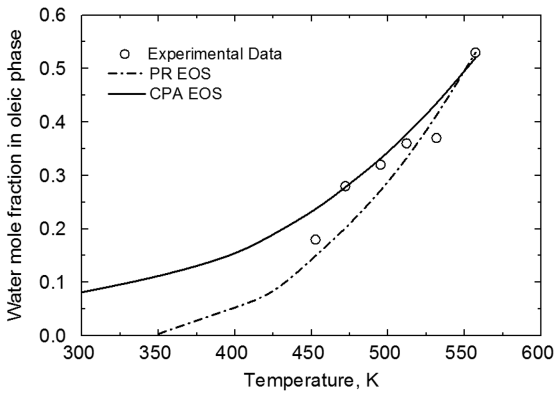

Figure 9. Comparison of the calculated total water content in the oleic phase in the water/Peace River bitumen mixture against the experimental data[57] for Case 3.

The PR EOS is taken from Venkatramani and Okuno.[43]

Table 9. Flash Results of the Water/Bitumen Mixture at 1400 kPa, 400 K and 1400 kPa, 465 K for Case 3: the CPA EOS Parameters Are Given in Table 8

		400 K, 1400 kPa			465 K, 1400 kPa	
Component	z	L_1	L_2	W	L_2	W
H_2O	0.7481	0.3628	0.0398	1	0.2645	1
PC1	0.0987	0.1864	0.4119	0	0.2883	0
PC2	0.0698	0.1136	0.3011	0	0.2038	0
PC3	0.0544	0.0797	0.2398	0	0.159	0
Asphaltene	0.0289	0.2576	0.0077	0	0.0844	0
Phase mole fraction		0.1065	0.1916	0.7019	0.3425	0.6575
Phase volume fraction		0.3034	0.6135	0.0876	0.9202	0.0798
Density (kg/m^3)		1016.87	816.68	934.89	843.24	865.15

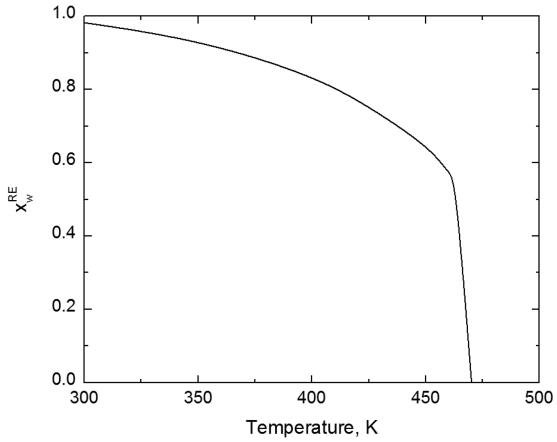

Figure 10. The change of x_w^{RE} with respect to temperature.

x_w^{RE} represents the ratio of the emulsified water content to the total water content in the oleic phase for Case 3. There is no emulsified water at temperatures higher than 465 K.

asphaltene forms cross-association with water and also because the solvation of PC1, PC2, PC3, and water. The L_1 phase is calculated to also contain *n*-butane in the presence of asphaltene and water. One way to interpret this calculation result is that the L_1 phase contains water-in-oil emulsion[21]. When the pressure is reduced to 3400 kPa, the L_2 phase is split into the V and L_2 phases, while the L_1 and W phases remain nearly unaffected.

These calculation results (Table 7) seem to be reasonable in comparison with the experimental observations. As shown in Gao et al.,[25] for example, the L_1 phase was between the L_2 and W phases in terms of density. Also, the L_1 phase was black, and the L_2 phase exhibited a lighter color than the L_1 phase. In Table 7, the L_1 phase represents the water/asphaltene emulsion, and the L_2 phase is substantially rich in *n*-butane; therefore, the L_2 phase is conceived to show a lighter color than the L_1 phase. These results show that the CPA EOS model offers a way to interpret the complex experimental results associated with water-asphaltene interaction.

Case 3: Water and peace river bitumen

Glandt and Chapman[57] measured water solubilities in Peace River bitumen near the V-L-W/L-W and L-W/L-V phase boundaries in the range from 452.65 to 557.15 K. The bitumen characterization with the CPA EOS is performed by use of the data given in Mehrotra and Svrcek.[58] Table 8 presents the resulting EOS parameters for four pseudo components, in which the heaviest component represents asphaltene.

As mentioned in New BIP Correlation for Water with Hydrocarbons for the CPA EOS section, the self-association of water and asphaltene, the cross-association between them, and the solvation between water and the other pseudo components (PC1, PC2, and PC3) are considered in the CPA EOS model. β^{AB} for PC1, PC2, and PC3, and ε^{AB} for asphaltene are adjusted to match the measured water solubility at 557.15 K, which is the highest temperature used for the experiment. The resulting value for β^{AB} is 0.02 for PC1, PC2, and PC3. The ε^{AB} parameter for asphaltene is set to 17.50 kPa·m^3·mol^{-1}.

Figure 9 presents the experimental water solubilities and calculations based on the CPA EOS (this research) and the PR EOS.[43] The solid curve was predicted by use of the parameters calibrated with the water solubility at 557.15 K. The AAD for water solubilities is 0.028 with the CPA EOS model and 0.038 with the PR EOS. The CPA EOS model gives higher water contents than the PR EOS model below 450 K. The PR EOS model gives no solubility of water in oil below 350 K, which is consistent with experimental results at low temperatures by Amani et al.[50] The experimental studies by Glandt and Chapman[57] and Gao et al.[25] indicated that water could come out of the oil phase to form water-in-oil emulsion with decreasing temperature. The water content in emulsion can be significantly higher than the solubilized water content in bitumen at low temperatures.[59] The current CPA EOS model captures the water solubility in bitumen at elevated temperatures, and the precipitation of water that forms water-in-oil emulsion at lower temperatures.

Table 9 shows the flash results of the water/Peace River bitumen mixture at 400 and 465 K. The mixture exhibits WL_1L_2 equilibrium at 400 K and WL_2 equilibrium at 465 K. At 400 K, the L_1 phase is rich in asphaltene and water, and considered to represent water-in-oil emulsion. The L_2 phase represents the bitumen-rich phase containing a smaller amount of water. At 465 K, only one oleic phase is calculated, resulting from the merging of the emulsion phase and bitumen-rich phase. The PR EOS model presented in Venkatramani and Okuno[43] gave only one oleic phase and one aqueous phase at 400 and 465 K because their EOS model was designed to represent only the solubility of water in oil, but not the emulsion resulting from associations of asphaltene and water.

The emulsified water content ($x_w^{Emulsion}$), the total water content (x_w^{Oleic}) in the oleic phases, and the ratio of $x_w^{Emulsion}$ to x_w^{Oleic} are defined as follows

$$x_w^{Emulsion} = \frac{x_{w-L1} x_{L1}}{x_{L1} + x_{L2}} \tag{19}$$

$$x_w^{Oleic} = \frac{x_{w-L1} x_{L1} + x_{w-L2} x_{L2}}{x_{L1} + x_{L2}} \tag{20}$$

$$x_w^{RE} = \frac{x_w^{Emulsion}}{x_w^{Oleic}} \tag{21}$$

where x_{L1} and x_{L2} refer to the mole fraction of the emulsion phase and the bitumen-rich phase, respectively; $x_{w\text{-}L1}$ and $x_{w\text{-}L2}$ refer to the water mole fraction in the emulsion phase and the bitumen-rich phase, respectively; x_w^{RE} represents the ratio of emulsified water content to the total water content in the oleic phase.

Table 10. Parameters for Water, Toluene, KU-Asphaltene, and OMV1 Asphaltene for Case 4: the Volume Shift Parameters Were Used to Match the Asphaltene Density 1.1 kg/m^3

Component	MW (g/mol)	T_C (K)	a_0 (kPa·m^6·mol^{-2})	b (m^3·mol^{-1})	κ	ε^{AB} (kPa·m^3·mol^{-1})	β^{AB}	$K_{w\text{-HC}}$	Volume shift
H_2O	18.02	647.3	0.00012	0.0000145	0.6735	16.655	0.0692	0.000	0
Toluene	92.14	591.7	0.002515	0.000104	0.8729	–	0.06	0.018	0
KU Asphaltene	1000	1040	0.0155	0.000562	2.486	25.0	0.05	−0.038	−0.000346
OMV1 Asphaltene	1000	1040	0.0155	0.000562	2.486	17.0	0.05	−0.038	−0.000346

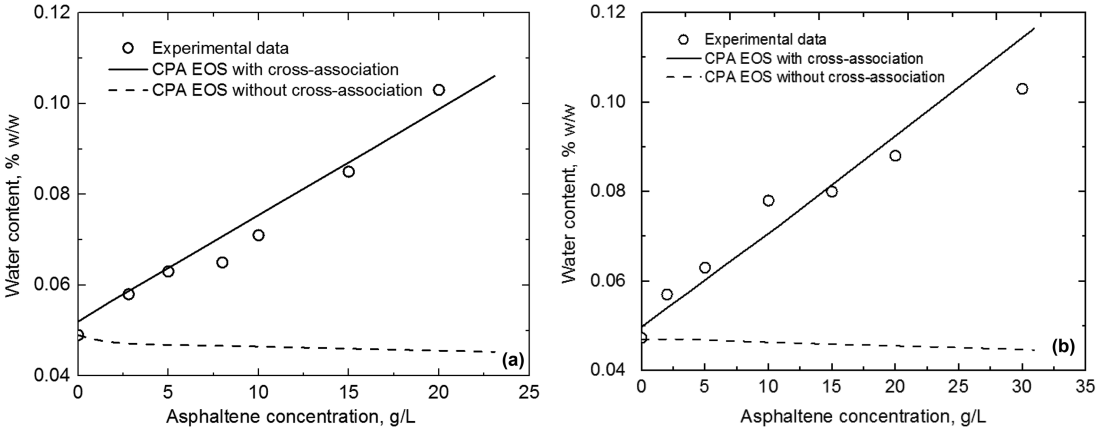

Figure 11. Comparison of calculated water solubilities in asphaltene-toluene solutions against experimental data for Case 4.

(a) Water solubilities in KU asphaltene-toluene solutions[60]; (b) water solubilities in OMV1-asphaltene/toluene solutions.

Figure 10 shows the variation of x_w^{RE} with temperature. It is shown that x_w^{RE} rapidly increases near 465 K, and then gradually increases from 0.56 to 0.98 from 460 to 300 K. This trend of x_w^{RE} with respect to temperature is in accordance with the observation that solubilized water in bitumen comes out of the solution as water-in-oil emulsion with decreasing temperature.[25,57] This example shows the additional flexibility that the CPA EOS offers for representation of water-asphaltene association.

Case 4: Water in asphaltene-toluene solutions

Andersen et al.[60] measured the water solubility in asphaltene/toluene solutions. They found that the water solubility increases with increasing asphaltene concentration in toluene. In this subsection, the CPA EOS is applied to represent the multiphase behavior observed for water/KU-asphaltene/toluene mixtures by Andersen et al.[60] and water/OMV1-asphaltene/toluene mixtures by Khvostichenko and Andersen.[61]

The self-association of water and asphaltene and the cross-association between water and asphaltene molecules are modeled. The solvation between toluene and water is also included in the model, which enables toluene to form cross-association with water molecules. As suggested by Kontogeorgis and Folas,[35] β^{AB} for toluene is set to 0.06. The BIP of water with toluene has been obtained by matching the water solubility in pure toluene, resulting in $k_{water\text{-}toluene} = 0.018$. The BIP of water with asphaltene is set to -0.038, by use of the new correlation presented in New BIP Correlation for Water with Hydrocarbons for the CPA EOS section. The other BIPs are set to zero.

In the absence of information regarding these asphaltene samples, except for the MW around 1000 g/mol, this subsection uses T_C, P_C, and ω for the asphaltene sample of Arya et al.[32] as the initial guesses for the properties of KU asphaltene and OMV1 asphaltene. Then, ε^{AB} for asphaltene is adjusted to match one measured water solubility for each asphaltene sample. The water solubility for KU asphaltene concentration, 6.29 g/L, and the OMV1 asphaltene concentration, 16.18 g/L, are used for calibration of the model. The volume shift method is used to adjust the density of the pure asphaltene, 1100 g/m^3 as given by Andersen et al.[60] The other data points are saved for testing the resulting CPA EOS models. The parameters for toluene, KU asphaltene, and OMV1 asphaltene are summarized in Table 10.

Figure 11 presents the comparison of calculated water solubilities in asphaltene-toluene solutions with the experimental data. Calculations are obtained in two ways: one with the asphaltene-water cross-association, and the other without the cross-association. The CPA EOS models represent reasonably the water solubilities, and the increasing water content with increasing asphaltene concentration in toluene. Figure 11 also shows that the calculated water solubility erroneously decreases with increasing asphaltene concentration in toluene if the asphaltene-water cross-association is not considered in the model.

Khvostichenko and Andersen[61] found that the number of water molecules bound to one asphaltene molecule (n_b) decreased from several water molecules to below unity with increasing asphaltene amount in toluene from 0.1 to 20 g/L. This tendency is also captured by the CPA EOS models. According to the difference between the water solubility in the pure toluene and that in the toluene-asphaltene solutions, n_b can be calculated as

$$n_b = \frac{x_w^{sat} - x_w^{tol}}{x_{asp}} \tag{22}$$

where x_w^{sat} refers to the mole fraction of saturation water in asphaltene-toluene solutions; x_w^{tol} refers to mole fraction of

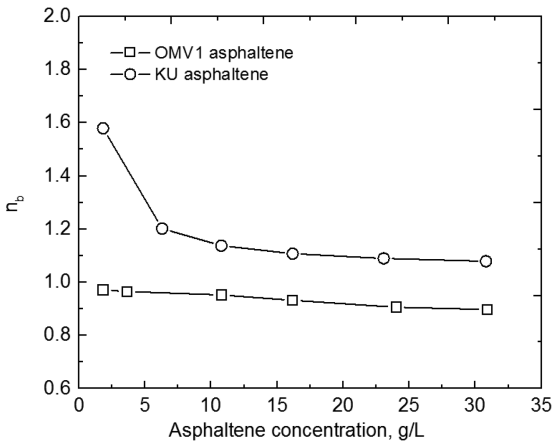

Figure 12. Change of the n_b with respect to the asphaltene concentration in asphaltene-toluene solutions for Case 4.

n_b refers to the number of water molecules bound to one asphaltene molecule.

Table 11. Flash Results for the OMV1-Asphaltene/Toluene/Water Mixtures at 102 kPa and 298 K for Case 4

	WL_2 equilibrium			WL_1L_2 equilibrium			
Component	z	L_2	W	z	L_1	L_2	W
H_2O	0.00990	0.00324	0.99999	0.00990	0.14180	0.00324	0.99999
Toluene	0.98922	0.99588	0.00001	0.98921	0.71753	0.99587	0.00001
Asphaltene	0.00088	0.00089	0.00000	0.00089	0.14067	0.00089	0.00000
Phase mole fraction	–	0.99332	0.00668	–	0.00003	0.99321	0.00666
Phase volume fraction	–	0.9990	0.0010	–	0.0000801	0.99893	0.00099
Density (kg/m^3)		766.35	1005.7		944.03	766.36	1005.7

saturation water in the pure toluene, and x_w^{tol} is set to 0.047%[60]; x_{asp} is the mole fraction of asphaltene in the solution.

Figure 12 shows the changes of n_b with the asphaltene concentration in asphaltene-toluene solutions. It shows that n_b decreases with increasing asphaltene concentration, as presented by Khvostichenko and Andersen.[61] These results can be interpreted as the formation of asphaltene aggregations at high asphaltene concentrations. For OMV1 asphaltene, n_b is calculated in the range of 1.0–1.6 from 1.8 to 31 g asphaltene in 1 L solutions. For KU asphaltene, n_b is calculated in the range of 0.88–0.98 from 1.8 to 31 g asphaltene in 1 L solutions.

Table 11 gives two examples of flash results of asphaltene/water/toluene mixtures. When the feed asphaltene concentration is 0.088 mol %, the mixture exhibits WL_2 equilibrium. However, when the feed asphaltene concentration increases to 0.089 mol %, an asphaltene-rich phase with a high water concentration separates from the toluene-rich phase, resulting in the coexistence of WL_1L_2 phases. Such WL_1L_2 results cannot be captured unless the thermodynamic model accounts for the water-asphaltene cross-association.

Conclusions

The CPA EOS was applied for the first time to model the strong interaction between water and asphaltene and its effects on the multiphase behavior for mixtures of water with asphaltene-containing reservoir oils. A new BIP correlation for water/*n*-alkane binaries for the CPA EOS was developed by matching three-phase coexistence curves measured by Brunner.[42] Then, a five-step procedure was developed to characterize mixtures of asphaltene-containing oil with water by using the CPA EOS. Experimental data available in the literature were used to characterize several asphaltene-containing oils with four pseudo components asphaltene and three non-self-associating components. The applicability of the resulting CPA EOS models were tested for representation of multiphase behavior (up to four equilibrium phases) involving water solubility in oil and water-asphaltene emulsion. Case studies were shown to demonstrate the importance of the cross-association between asphaltenes and water for such complex multiphase behavior. Conclusions are as follows:

1. The new BIP correlation enables the CPA EOS to accurately represent the three-phase coexistence and the water solubility in *n*-alkane for water/*n*-alkane binaries. Using the CPA EOS with the new BIP correlation, the thee-phase curve asymptotically approaches the vapor pressure of water as the *n*-alkane component becomes heavier. The new correlation gives the BIP for water that decreases from 0.306 to −0.0378 for *n*-C_4 to *n*-C_{36}. For *n*-alkanes heavier than *n*-C_{36}, the BIP is calculated as a constant value of −0.0380.

2. The CPA EOS was successfully applied to represent the water concentrations in asphaltene solutions in toluene published in the literature. The cross-association between water and asphaltene molecules, which was implemented with the CPA EOS for the first time, results in the formation of an asphaltene-rich emulsion phase. The emulsion contributes to the increased water content in asphaltene-toluene solutions with increasing asphaltene concentration.

3. The CPA EOS was able to calculate the smooth transition from solubilized water at high temperatures to emulsified water in bitumen at low temperatures, yielding a more accurate method to estimate water contents in bitumen for a wide range of temperatures. The emulsified water fraction increases from zero to near unity with decreasing temperature for the case studied.

4. The CPA EOS reasonably represents the complex phase boundaries observed for an *n*-butane/bitumen/water mixture from WL_2, to WL_1L_2, to WL_1L_2V with decreasing pressure. When the mixture exhibits WL_1L_2V or WL_1L_2 equilibrium, the *n*-butane solvent extracts most of the aromatic hydrocarbons from bitumen, while almost all of the asphaltene exists in the emulsion phase due to the strong interaction between water and asphaltene molecules. The PR EOS could not correlate the transition from WL_2 to WL_1L_2 likely because it is difficult for the PR EOS to account for the cross-association of asphaltene and water.

Acknowledgments

This study was financially supported by the National Natural Science Foundation of China (No. 51504206). We gratefully acknowledge the financial support from Japan Canada Oil Sands. for this research. Okuno holds the Pioneer Corporation Faculty Fellowship in Petroleum Engineering at The University of Texas at Austin.

Notation

C_1, C_2, C_3 = coefficients for BIP correlation
A, B = parameters in the SRK EOS
L = oleic phase
P = pressure
R = gas constant
T = temperature
V = vapor phase
Z = compressibility factor
W = aqueous phase
x = mole fraction
a = energy parameter
a_0 = energy parameter
b = co-volume
g = hard sphere radial distribution function
i, j = indices
k = binary interaction parameter
n = number
z = overall composition

Greek letters

β = association volume
Δ = association strength
ε = association energy
κ = energy parameter
ρ = molar density
ω = acentric factor
φ = fugacity coefficient

Subscripts

A_i = active association site A on molecule i;
B_j = active association site A on molecule i;
HC = hydrocarbon
L = liquid phase
V = vapor phase
b = bound molecule
c = critical condition
RE = relative value
sat = saturation condition
tol = toluene
w = water

Literature Cited

1. Van Konynenburg PH. *Critical Lines and Phase Equilibria in Binary Mixtures* (PhD dissertation). Los Angeles: University of California, 1968.
2. Scott RL, van Konynenburg PH. Static properties of solutions. Van der Waals and related models for hydrocarbon mixtures. *Discuss Faraday Soc*. 1970;49:87–97. doi:10.1039/DF9704900087
3. Konynenburg PHV, Scott RL. Critical lines and phase equilibria in binary van der Waals mixtures. *Phil Trans R Soc A*. 1980; 298(1442):495–540. doi:10.1098/rsta.1980.0266
4. Sharma AK, Patil SL, Kamath VA, Sharma GD. Miscible displacement of heavy west sak crude by solvents in slim tube. Paper SPE-18761-MS presented at SPE California Regional Meeting, SPE, Bakersfield, CA, April 5–7, 1989. doi:10.2118/18761-MS
5. Khan SA, Pope GA, Sepehrnoori K. Fluid characterization of three-phase CO_2/oil mixtures. Paper SPE-24130-MS presented at SPE/DOE Enhanved Oil Recovery Symposium, SPE, Tulsa, OK, April 22–24, 1992. doi:10.2118/24130-MS
6. Creek JL, Sheffield JM. Phase behavior, fluid properties, and displacement characteristics of Permian Basin reservoir fluid/CO_2 Systems. *SPE Res Eng*. 1993; 8(01): 34–42. doi:10.2118/20188-PA
7. Godbole SP, Thele KJ, Reinbold EW. EOS modeling and experimental observations of three-hydrocarbon-phase equilibria. *SPE Res Eng*. 1995;10(02):101–108. doi:10.2118/24936-PA
8. Mohanty KK, Masino WH Jr, Ma TD, Nash LJ. Role of three-hydrocarbon-phase flow in a gas displacement process. *SPE Res Eng*. 1995;10(03):214–221. doi:10.2118/130802-PA.9
9. Gregorowicz J, de Loos TW. Modelling of the three phase LLV region for ternary hydrocarbon mixtures with the Soave-Redlich-Kwong equation of state. *Fluid Phase Equilibr*. 1996;118(1):121–132. doi:10.1016/0378-3812(95)02845-5
10. Bluma M, Deiters UK. A classification of phase diagrams of ternary fluid systems. *Phys Chem Chem Phys*. 1999;1(18):4307–4313. doi:10.1039/A904863D
11. Gauter K, Heidemann RA, Peters CJ. Modeling of fluid multiphase equilibria in ternary systems of carbon dioxide as the near-critical solvent and two low-volatile solutes. *Fluid Phase Equilibr*. 1999; 158–160:133–141. doi:10.1016/S0378-3812(99)00122-3
12. Mushrif SH, Phoenix AV. Effect of Peng−Robinson binary interaction parameters on the predicted multiphase behavior of selected binary systems. *Ind Eng Chem Res*. 2008;47(16):6280–6288. doi:10.1021/ie800599t
13. Okuno R, Xu Z. Efficient displacement of heavy oil by use of three hydrocarbon phases. *SPE J*. 2014;19(05):956–973. doi:10.2118/165470-PA
14. Kumar A, Okuno R. A new algorithm for multiphase fluid characterization for solvent injection. *SPE J*. 2016;21(05):1688–1704. doi:10.2118/175123-PA
15. Wang D, Lin M, Dong Z, Li L, Jin S, Pan D, Yang Z. Mechanism of high stability of water-in-oil emulsions at high temperature. *Energy Fuels*. 2016;30(3):1947–1957. doi:10.1021/acs.energyfuels.5b02203
16. Peng DY, Robinson DB. A new two-constant equation of state. *Ind Eng Chem Funda*. 1976;15(1):59–64. doi:10.1021/i160057a011
17. Robinson DB, Peng DY. *The Characterization of the Heptanes and Heavier Fractions for the GPA Peng–Robinson Programs* (Research report RR-28). Tulsa, OK: Gas Processors Association, 1978.
18. Soave G. Equilibrium constants from a modified Redlich-Kwong equation of state. *Chem Eng Sci*. 1972;27(6):1197–1203. doi:10.1016/0009-2509(72)80096-4
19. Chang Y-B. *Development and Application of an Equation of State Compositional Simulator* (PhD dissertation). Austin: University of Texas at Austin, 1990.
20. Chang Y-B, Pope GA, Sepehrnoori K. A higher-order finite-difference compositional simulator. *J. Petro Sci Eng*. 1990;5(1):35–50. doi:10.1016/0920-4105(90)90004-M
21. Aslan S, Firoozabadi A. Effect of water on deposition, aggregate size, and viscosity of asphaltenes. *Langmuir*. 2014;30(13):3658–3664. doi:10.1021/la404064t
22. Nasrabadi H, Moortgat J, Firoozabadi A. New three-phase multicomponent compositional model for asphaltene precipitation during CO_2 injection using CPA-EOS. *Energy Fuels*. 2016;30(4):3306–3319. doi:10.1021/acs.energyfuels.5b02944
23. Qin X, Wang P, Sepehrnoori K, Pope GA. Modeling asphaltene precipitation in reservoir simulation. *Ind Eng Chem Res*. 2000;39(8): 2644–2654. doi:10.1021/ie990781g
24. Mohebbinia S, Sepehrnoori K, Johns RT, Kazemi A, Korrabi N. Simulation of asphaltene precipitation during gas injection using PC-SAFT EOS. Paper SPE-170697-MS presented at SPE Annual Technical Conference and Exhibition, SPE, Amsterdam, October 27–29, 2014. doi:10.2118/170697-MS
25. Gao J, Okuno R, Li HA. An experimental study of multiphase behavior for n-butane/Bitumen/water mixtures. *SPE J*. 2017;22(03): 0783–0798. doi:10.2118/180736-PA
26. Kontogeorgis GM, Voutsas EC, Yakoumis IV, Tassios DP. An equation of state for associating fluids. *Ind Eng Chem Res*. 1996;35(11): 4310–4318. doi:10.1021/ie9600203
27. Li Z, Firoozabadi A. Cubic-plus-association equation of state for asphaltene precipitation in live oils. *Energy Fuels*. 2010;24(5):2956–2963. doi:10.1021/ef9014263
28. Li Z, Firoozabadi A. Modeling asphaltene precipitation by n-alkanes from heavy oils and bitumens using cubic-plus-association equation of state. *Energy Fuels*. 2010;24(2):1106–1113. doi:10.1021/ef9009857
29. Shirani B, Nikazar M, Mousavi-Dehghani SA. Prediction of asphaltene phase behavior in live oil with CPA equation of state. *Fuel*. 2012;97:89–96. doi:10.1016/j.fuel.2012.02.016
30. Zhang X, Pedrosa N, Moorwood T. Modeling asphaltene phase behavior: Comparison of methods for flow assurance studies. *Energy Fuels*. 2012;26(5):2611–2620. doi:10.1021/ef201383r
31. AlHammadi AA, Vargas FM, Chapman WG. Comparison of cubic-plus-association and perturbed-chain statistical associating fluid theory methods for modeling asphaltene phase behavior and pressure–volume–temperature properties. *Energy Fuels*. 2015;29(5):2864–2875. doi:10.1021/ef502129p
32. Arya A, von Solms N, Kontogeorgis GM. Determination of asphaltene onset conditions using the cubic plus association equation of state. *Fluid Phase Equilibr*. 2015;400:8–19. doi:10.1016/j.fluid.2015.04.032
33. Yan W, Kontogeorgis GM, Stenby EH. Application of the CPA equation of state to reservoir fluids in presence of water and polar chemicals. *Fluid Phase Equilibr*. 2009;276(1):75–85. doi:10.1016/j.fluid.2008.10.007
34. Zirrahi M, Hassanzadeh H, Abedi J. Prediction of water solubility in petroleum fractions and heavy crudes using cubic-plus-association equation of state (CPA-EoS). *Fuel*. 2015;159:894–899. doi:10.1016/j.fuel.2015.07.058
35. Kontogeorgis GM, Folas GK. *Thermodynamic Models for Industrial Applications: From Classical and Advanced Mixing Rules to Association Theories*. New York: John Wiley & Sons (Reprint), 2009.
36. Chapman WG, Gubbins KE, Jackson G, Radosz M. New reference equation of state for associating liquids. *Ind Eng Chem Res*. 1990; 29(8):1709–1721. doi:10.1021/ie00104a021
37. Folas GK, Kontogeorgis GM, Michelsen ML, Stenby EH. Application of the cubic-plus-association (CPA) equation of state to complex mixtures with aromatic hydrocarbons. *Ind Eng Chem Res*. 2006; 45(4):1527–1538.
38. Michelsen ML. Robust and efficient solution procedures for association models. *Ind Eng Chem Res*. 2006;45(25):8449–8453. doi:10.1021/ie060029x
39. Michelsen ML. The isothermal flash problem. Part I. Stability. *Fluid Phase Equilibr*. 1982;9(1):1–19. doi:10.1016/0378-3812(82)85001-2

40. Michelsen ML. The isothermal flash problem. Part II. Phase-split calculation. *Fluid Phase Equilibr*. 1982;9(1):21–40. doi:10.1016/0378-3812(82)85002-4
41. Okuno R, Johns R, Sepehrnoori K. A new algorithm for Rachford-Rice for multiphase compositional simulation. *SPE J*. 2010;15(02):313–325. doi:10.2118/117752-PA
42. Brunner E. Fluid mixtures at high pressures IX. Phase separation and critical phenomena in 23 (n-alkane+ water) mixtures. *J Chem Thermodyn*. 1990;22(4):335–353. doi:10.1016/0021-9614(90)90120-F
43. Venkatramani A, Okuno R. Characterization of water-containing reservoir oil using an EOS for steam injection processes. *J Nat Gas Sci Eng*. 2015;26:1091–1106. doi:10.1016/j.jngse.2015.07.036
44. Skripka VG. Solubility of water in normal alkanes at elevated temperatures and pressures. *Chem Technol Fuels Oils*. 1979;15(2):88–90. doi:10.1007/BF00749406
45. Heidman JL, Tsonopoulos C, Brady CJ, Wilson GM. High-temperature mutual solubilities of hydrocarbons and water. Part II: Ethylbenzene, ethylcyclohexane, and n-octane. *AIChE J*. 1985;31(3):376–384. doi:10.1002/aic.690310304
46. Tsonopoulos C, Wilson GM. High-temperature mutual solubilities of hydrocarbons and water. Part I: Benzene, cyclohexane and n-hexane. *AIChE J*. 1983;29(6):990–999. doi:10.1002/aic.690290618
47. PVTsim Nova (Version 3.0) [Computer software]. 2017. Lyngby: Calsep A/S. Retrieved from https://www.pvtsimnova.com/.
48. Péneloux A, Rauzy E, Fréze R. A consistent correction for Redlich-Kwong-Soave volumes. *Fluid Phase Equilibr*. 1982;8(1):7–23. doi:10.1016/0378-3812(82)80002-2
49. Amani MJ, Gray MR, Shaw JM. Phase behavior of Athabasca bitumen + water mixtures at high temperature and pressure. *J. Supercrit Fluids*. 2013;77:142–152. doi:10.1016/j.supflu.2013.03.007
50. Amani MJ, Gray MR, Shaw JM. Volume of mixing and solubility of water in Athabasca bitumen at high temperature and pressure. *Fluid Phase Equilibr*. 2013;358:203–211. doi:10.1016/j.fluid.2013.07.021
51. Badamchi-Zadeh A, Yarranton HW, Svrcek WY, Maini BB. Phase behaviour and physical property measurements for VAPEX solvents: Part I. Propane and Athabasca bitumen. *J Can Pet Technol*. 2009;48(01):54–61. doi:10.2118/09-01-54
52. Nasr TN, Beaulieu G, Golbeck H, Heck G. Novel expanding solvent-SAGD process "ES-SAGD." *J Can Pet Technol*. 2003;42(01):13–16. doi:10.2118/03-01-TN
53. Nasr TN, Ayodele OR. New hybrid steam-solvent processes for the recovery of heavy oil and bitumen. Paper SPE-101717-MS presented at Abu Dhabi International Petroleum Exhibition and Conference, SPE, Abu Dhabi, November 5–8, 2006. doi:10.2118/101717-MS
54. Gupta S, Gittins S, Picherack P. Field implementation of solvent aided process. *J Can Pet Technol*. 2005;44(11):8–13. doi:10.2118/05-11-TN1
55. Li W, Mamora DD, Li Y. Solvent-type and-ratio impacts on solvent-aided SAGD process. *SPE Res Eval Eng*. 2011;14(03):320–331. doi:10.2118/130802-PA
56. Venkatramani A, Okuno R. Compositional mechanisms in steam-assisted gravity drainage and expanding-solvent steam-assisted gravity drainage with consideration of water solubility in oil. *SPE Res Eval Eng*. 2017;20(03):681–697. doi:10.2118/180737-PA
57. Glandt CA, Chapman WG. The effect of water dissolution on oil viscosity. *SPE Res Eng*. 1995;10(01):59–64. doi:10.2118/24631-PA
58. Mehrotra AK, Svrcek WY. Viscosity, density and gas solubility data for oil sand bitumens. Part I: Athabasca bitumen saturated with CO and C_2H_6. *AOSTRA J Res*. 1985;1(4):263–268.
59. Spiecker PM, Gawrys KL, Trail CB, Kilpatrick PK. Effects of petroleum resins on asphaltene aggregation and water-in-oil emulsion formation. *Colloids Surf Physicochem Eng Aspects*. 2003;220(1–3):9–27. doi:10.1016/S0927-7757(03)00079-7
60. Andersen SI, del Rio JM, Khvostitchenko D, Shakir S, Lira-Galeana C. Interaction and solubilization of water by petroleum asphaltenes in organic solution. *Langmuir*. 2001;17(2):307–313. doi:10.1021/la000871m
61. Khvostichenko DS, Andersen SI. Interactions between asphaltenes and water in solutions in toluene. *Energy Fuels*. 2008;22(5):3096–3103. doi:10.1021/ef700757h

Manuscript received Oct. 14, 2017, and revision received Mar. 5, 2018.